

A coupled petrological–tectonic model for sedimentary basin evolution: the influence of metamorphic reactions on basin subsidence

K. Petrini, J. A. D. Connolly* and Yu. Yu. Podladchikov

Earth Sciences Department, ETH Zurich, Sonneggstr. 58092 Zurich, Switzerland

ABSTRACT

The lithosphere is subject to fluctuations in temperature and pressure during the formation of sedimentary basins. These fluctuations cause metamorphic reactions that change the density of the lithosphere, which, in turn, influences basin subsidence. This contribution develops a model for sedimentary basin formation to assess the importance of this coupling. The model shows that basin subsidence is significantly affected by metamorphic densification. Compared to results obtained with cruder density models, metamorphic densification accelerates subsidence in the initial post-rifting stages as garnet becomes

stable over an increasing depth interval within the mantle, an effect that amplifies the crust–mantle density contrast. For models with an extraordinarily cold lithosphere, uplift is generated as a late stage of basin evolution. In general, subsidence is not smooth but occurs instead in small steps reflecting periods of accelerated/decelerated subsidence. For typical crustal thicknesses, subsidence is controlled largely by reactions in the mantle, and particularly those determining garnet stability.

Terra Nova, 13, 354–359, 2001

Introduction

During the tectonic rifting that leads to the formation of a sedimentary basin, the lithosphere undergoes rapid heating and decompression. Subsequently, the geotherm evolves toward a steady-state thermal gradient as the lithosphere cools. The changes in temperature and pressure during this evolution cause metamorphic reactions that affect the bulk physical properties of the lithosphere. Sedimentary basin subsidence is dependent on these properties, particularly density, and it is therefore to be expected that it will be affected by metamorphic reactions. The potential influence of metamorphic reactions on subsidence was recognized several decades ago (Lovering, 1958; Kennedy, 1959) and some subsequent authors have attributed subsidence entirely to metamorphic densification (e.g. Middleton, 1980; Artyushkov, 1983; Artyushkov *et al.*, 1991; Hadmani *et al.*, 1991; Naimark and Ismail-Zadeh, 1995; Lobkovsky *et al.*, 1996; Ismail-Zadeh *et al.*, 1997). In recent work, metamorphic densification has been taken into consideration both in the context

of compressional tectonic settings (Bousquet *et al.*, 1997) and within the framework of extensional settings relevant to basin formation (Podladchikov *et al.*, 1994; Yamasaki and Nakada, 1997). The latter two papers consider a schematic discontinuous spinel–garnet reaction in the mantle without specifying the chemical system considered; therefore, the pressure–temperature conditions for the reaction are poorly constrained. In nature, the reaction is continuous, and therefore its realistic simulation requires the use of a petrological model incorporating solid solution behaviour. An additional limitation of simplified models is that it is not possible to determine *a priori* which reactions have important effects on subsidence; this is because the importance of a reaction with a large density difference may be overridden by the cumulative effect of several reactions with smaller density changes, or by a reaction with smaller density change but stronger depth dependence, which thus affects a larger portion of the lithosphere.

In order to determine the importance of metamorphic densification during sedimentary basin formation, it is crucial to take into consideration the bulk of the reactions likely to occur within the lithosphere. The present contribution presents the results of a coupled petrological–geodynamic model for basin formation in which the petrological component is used to

establish the variation in rock density caused by mineral transformations. The petrological calculations are made for realistic approximations of natural rock compositions and account for mineral solution behaviour. This model is then used to evaluate the effects of the density changes in the context of a simple basin model after McKenzie (1978).

Petrological model

The relative proportions, compositions and densities of the stable minerals as a function of pressure, temperature and bulk composition were computed from thermodynamic data with a free-energy minimization program described in detail elsewhere (Connolly, 1990; Connolly and Petrini, 2002). This computational strategy differs from more traditional thermodynamic approaches used previously to quantify lithospheric density (e.g. Sobolev and Babeyko, 1994) in that the nonlinear free-energy composition surfaces of solution phases are approximated by inscribed polyhedra. As a consequence of this approximation, phase diagram sections defined by environmental variables such as pressure and temperature are discretized by a polygonal mesh. This representation is particularly convenient for geodynamic modelling because once such a mesh has been computed all aspects of the thermodynamic state

*Correspondence: J. A. D. Connolly, Institut für Mineralogie and Petrographie, Earth Sciences Department, ETH Zurich, Sonneggstr. 58092 Zurich, Switzerland. Tel.: +41 1632 78 04; fax: +41 1632 10 88; e-mail: james.connolly@erdw.ethz.ch

of the system can be recovered easily at any point within the mesh by automated procedures. For present purposes, fertile lherzolithic and granodioritic bulk chemical compositions were taken to represent the compositions of the mantle and crust, respectively (Table 1). Thermodynamic data provided by Holland and Powell (1998) were used for all end-member phase compositions, the mineral solution models employed are detailed in Table 2, and the accuracy of the discretization was specified so as to resolve mineral compositions with a maximum error of 3 mol%. Calculations for the crust were performed assuming water saturation, whereas the mantle was assumed to be anhydrous. The stable mineral assemblages as a function of pressure (P) and temperature (T) for the two bulk compositions are shown in Fig. 1. The computed densities are shown in Fig. 2. Choosing a granodioritic composition for the crust leads to relatively low densities at eclogite facies conditions compared to those for a more mafic crustal model (e.g. Artyushkov *et al.*, 1991; Lobkovsky *et al.*, 1996; Bousquet *et al.*, 1997). This effect is of little consequence for results reported here, because the model crust has a maximum thickness of 35 km.

Basin model

Basin subsidence is calculated using a 1D implicit finite-difference model. The thermal evolution of the lithosphere is computed from the heat conduction–advection equation with radioactive heat production:

$$\frac{\partial T}{\partial t} + v_z \frac{\partial T}{\partial z} = \frac{k}{\rho c} \frac{\partial^2 T}{\partial z^2} + \frac{A}{\rho c}, \quad (1)$$

Table 1 Crust and mantle model compositions (weight percentage, Taylor and McLennan, 1985)

	Crust	Mantle
SiO ₂	66.0	45.0
Al ₂ O ₃	15.2	3.3
FeO	4.5	8.0
MgO	2.2	36.3
CaO	4.2	2.6
Na ₂ O	3.9	0.34
K ₂ O	3.4	0
H ₂ O	saturated	0

Table 2 Mineral solution notation, formulae and model sources (see table footnote). The compositional variables w , x , y , and z may vary between zero and unity and are determined as a function of pressure and temperature by free-energy minimization

Solution	Symbol	Formula	Source
Amphibole	Amph	Ca ₂ Na _w Mg _x Fe _{1-x} Al _{3w+4y} Si _{8-2w-2y} O ₂₂ (OH) ₂	1
Biotite	Bio	KMg _{(3-y)x} Fe _{(3-y)(1-x)} Al _{1+2y} Si _{3-y} O ₁₀ (OH) ₂	1
Chlorite	Chl	Mg _{(5-y+z)x} Fe _{(5-y+z)(1-x)} Al _{2(1+y+z)} Si _{3-y+z} O ₁₀ (OH) ₈	2
Clinopyroxene	Cpx	Na _{1-y} Ca _y Mg _x Fe _{1-yx} Al ₂ Si ₂ O ₆	3
Glaucofane	Gl	Ca _{2-2z} Na ₂ Mg _x Fe _(1-x) Al _{3w+4y} Si _{8-2w-2y} O ₂₂ (OH) ₂	1
Garnet	Gt	Fe _{3x} Ca _{3y} Mg _{31-x-y} Al ₂ Si ₃ O ₁₂	1
Alkali feldspar	Kf	Na _x K _y AlSi ₃ O ₈	4
Olivine	Ol	Mg _x Fe _{1-x} SiO ₄	1
Orthopyroxene	Opx	Mg _{x(2-y)} Fe _{(1-x)(2-y)} Al _{2y} Si _{2-y} O ₆	1
Phengite	Phen	K _x Na _{1-x} Mg _y Fe _z Al _{3-2(y+z)} Si _{3+y+z} O ₁₀ (OH) ₂	1, 5
Plagioclase	Pl	Na _x Ca _{1-x} Al _{2-x} Si _{2+x} O ₈	6
Sanidine	San	Na _x K _y AlSi ₃ O ₈	4
Spinel	Sp	Mg _x Fe _{1-x} AlO ₃	1

Sources: 1, Holland and Powell (1998); 2, Holland *et al.* (1998); 3, Gasparik (1985a,b); 4, Thompson and Waldbaum (1969); 5, Chatterjee and Froese (1975); 6, Newton *et al.* (1980).

where t is time v_z is vertical velocity, k is thermal diffusivity, ρ is density, c is specific heat per unit mass, A is volumetric heat production and z is the coordinate in the vertical direction. The vertical velocity v_z is calculated to correspond to:

$$v_z = -(\log \delta / t_{\text{rift}})z, \quad (2)$$

where δ is the ratio between initial lithospheric thickness and post-rift lithospheric thickness and t_{rift} is the total time during which the basin is stretching. The parameter values adopted for the calculations are listed in Table 3.

Initially the model basin consists of two layers: crust and mantle. During rifting the base of the model is infilled with asthenospheric material where as sediments (with a density of 2200 kg m⁻³) are added at the upper boundary to compensate for subsidence. Calculations are performed using both a ‘conventional’ model and the ‘real’ densities obtained from the petrological model. In the ‘conventional’ model densities for the crust and mantle are calculated as:

$$\rho = \rho_0(1 - \alpha T + \beta P), \quad (3)$$

where ρ_0 is the reference density for the lithology, α is the thermal expansivity and β is the compressibility (Table 3). Tectonic subsidence is computed iteratively in order to preserve isostatic equilibrium. The results obtained numerically for the conventional model were verified by

comparison with the analytical solution (McKenzie, 1978).

Results

The final subsidence for the ‘real’ density model is given approximately by the ‘conventional’ model (3) with a reference mantle density of 3340 kg m⁻³ and density contrast $\Delta\rho = \rho_{\text{mantle}} - \rho_{\text{crust}}$ of 590 kg m⁻³ (Fig. 3). However, in detail, the ‘real-density’ model evolution reflects the continuous variation in both absolute densities and density contrast between mantle and crust. The density contrast increases progressively, enhancing subsidence as an increasing portion of the mantle reaches conditions of garnet stability. The resulting subsidence is not smooth, but occurs instead in small steps reflecting periods of accelerated/decelerated subsidence (Fig. 3). The steps correspond to periods in which the geotherm intersects the conditions for garnet-forming reactions at temperatures characterized by important density contrasts, e.g. ~ 800 °C, ~ 500 °C (Fig. 2). Subsidence is also affected by the lower boundary temperature imposed for the model. To illustrate this effect, five experiments were performed with different boundary temperatures (Fig. 4). The first four experiments, with temperatures ranging from 1400 to 900 °C, result in final subsidence differing by about 200 m. Greater deviations occur in the last case, which presents an especially cold scenario

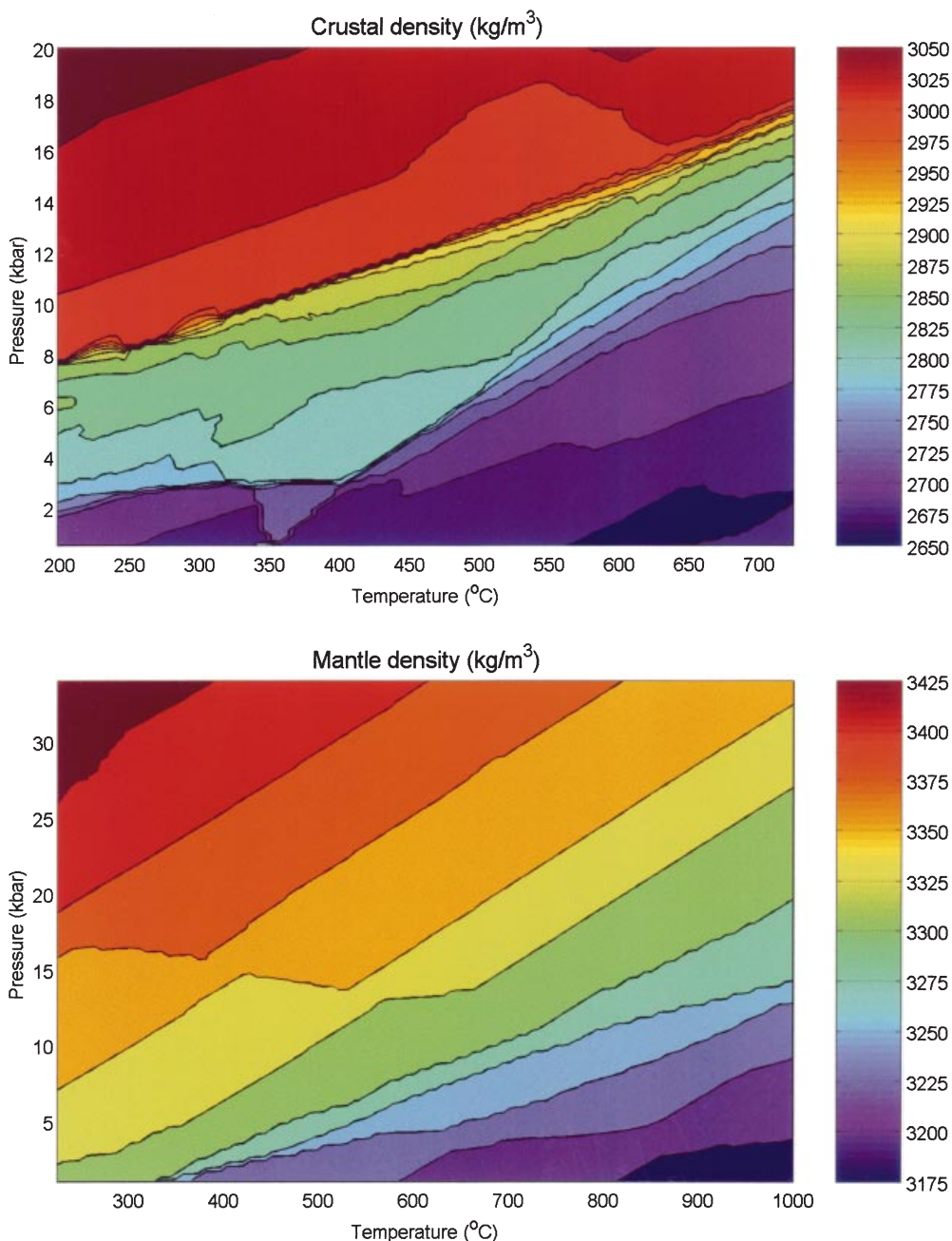


Fig. 2 False-colour density maps computed by free-energy minimization for mantle and crust model compositions (Table 1). The contour interval for both maps is 25 kg m⁻³.

Table 3 Model parameters

Parameter	Symbol	Value
Thermal diffusivity	<i>k</i>	1 × 10 ⁻⁶ (m ² s ⁻¹)
Specific heat per unit mass	<i>c</i>	1 × 10 ³ (J kg ⁻¹ K ⁻¹)
Crustal volumetric heat production	<i>A</i>	1 × 10 ⁻⁶ (W m ⁻³)
Isobaric thermal expansivity	α	3 × 10 ⁻⁵ K ⁻¹
Isothermal compressibility	β	1 × 10 ⁻¹¹ Pa ⁻¹

at equilibrium pressure and temperature conditions irrespective of reaction kinetics or of the previous history of the rock (e.g. Bousquet *et al.*, 1997). In nature, reactions may occur at pressures and temperatures different from those predicted by an equilibrium model. Additionally, crustal metamorphism is generally not isochemical, most notably with regard to volatile components and it is to be

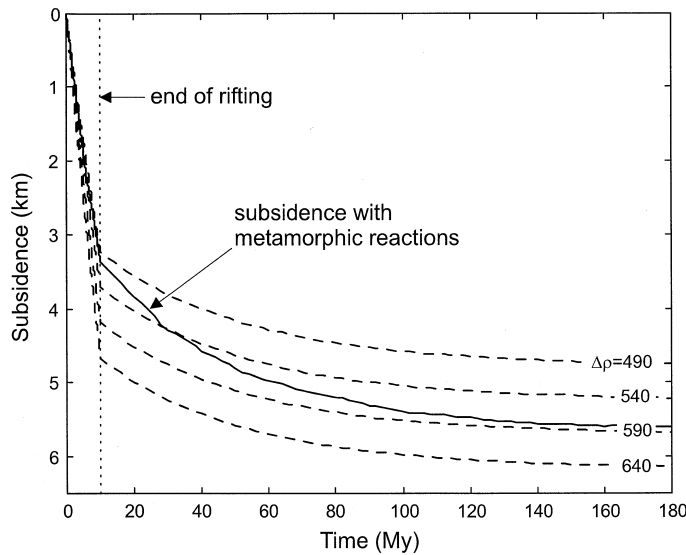


Fig. 3 Tectonic subsidence as a function of time for $\delta = 1.5$ (eqn 2), initial crustal thickness = 30 km, lithospheric thickness = 125 km, bottom temperature = 1000 °C, sediment density = 2200 kg m⁻³. Other parameters as in Table 3. The solid curve corresponds to the subsidence curve obtained with densities from the petrological model. Dashed curves correspond to subsidence obtained with assumed a reference mantle density (ρ_0) of 3340 kg m⁻³ and density contrasts between crust and mantle of 490, 540, 590 and 640 kg m⁻³, corrected for thermal and pressure effects as in (3).

expected that volatile loss during prograde metamorphism may hinder retrograde hydration (Connolly and Thompson, 1989; Rubie, 1990). To approximate this effect, an experiment was carried out in which rehydration reactions were suppressed: it was

found that assemblages with the lowest water content achieved by the rocks were preserved throughout the subsequent history. In the present model, this effect is only important in the crust as the mantle is anhydrous. For average crustal thickness,

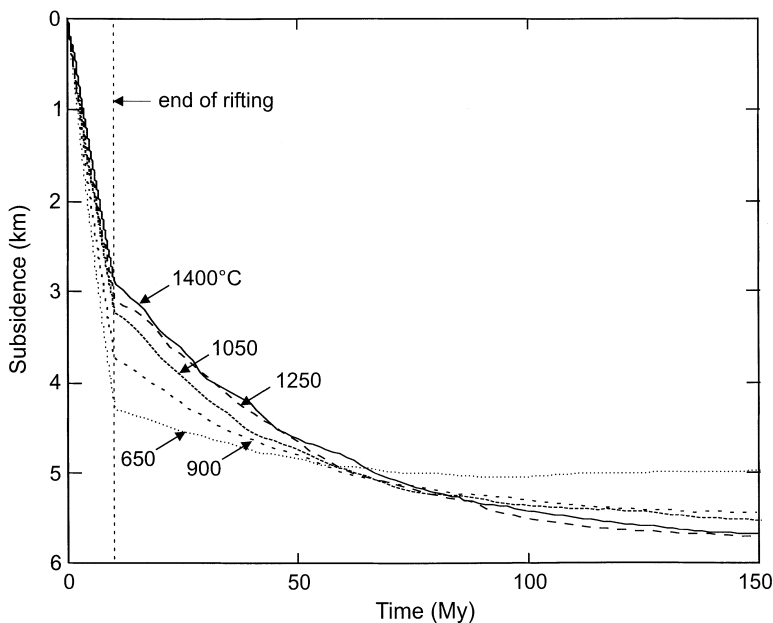


Fig. 4 Tectonic subsidence as a function of time and bottom temperature with all other parameters as indicated for Fig. 3.

the resulting subsidence curves are not affected by the omission of retrogressive reactions. This result reiterates the relative importance of mantle reactions.

It has been proposed previously that sharp steps in subsidence curves – in some cases even leading to phases of uplift – result from discontinuous mantle reactions (e.g. Podladchikov *et al.*, 1994; Yamasaki and Nakada, 1997). With the present model, reaction-related uplift is observed only in extreme cases (cold scenarios) and only in the later stages of basin evolution; furthermore, the steps in the subsidence curves are smooth compared with those of discontinuous models. Nevertheless, the overall effects are still important and, as reactions are an almost inevitable result of variations in pressure and temperature, exclusion of these effects will result in inaccurate subsidence curves.

Conclusion

Incorporation of the densification effects caused by metamorphic reactions in models for sedimentary basin formation lead to significant changes in predicted subsidence curves compared to those obtained with the conventional density model. Although these effects are quantitatively significant, metamorphic densification does not substantially alter the qualitative behaviour predicted by the conventional model. Metamorphic reactions cause faster subsidence rates in the initial stages of post-rift subsidence. This behaviour is induced by an increase in density contrast between the crust and the mantle. In the case of cold lithosphere, uplift is observed as a late stage of basin evolution. The subsidence curves produced with the density model presented herein show periods of faster and slower subsidence caused by variations in the density across mineral stability fields. For typical crustal thickness, subsidence is controlled largely by the reactions occurring in the mantle, and particularly by those affecting garnet stability.

Acknowledgements

We are grateful to Kurt Stuewe and an anonymous reviewer for constructive

comments. This work was supported by research funds granted by the Swiss Federal Institute of Technology to Alan B. Thompson and Jean-Pierre Burg (ETH Project 0-20272-96).

References

- Artyushkov, E.V., 1983. *Developments in Geotectonics*. Elsevier, Amsterdam.
- Artyushkov, E.V., Baer, M.A., Letnilov, F.A. and Ruzhich, V.V., 1991. On the mechanism of graben formation. *Tectonophysics*, **197**, 99–115.
- Bousquet, R., Goffe, B., Henry, P., Le Pichon, X. and Chopin, C., 1997. Kinematic, thermal and petrological model of the Central Alps; Lepontine metamorphism in the upper crust and eclogitisation of the lower crust. *Tectonophysics*, **273**, 105–127.
- Chatterjee, N.D. and Froese, E., 1975. A thermodynamic study of the pseudobinary join muscovite-paragonite in the system $KAlSi_3O_8$ - $NaAlSi_3O_8$ - Al_2O_3 - SiO_2 - H_2O . *Am. Miner.*, **60**, 985–993.
- Connolly, J.A.D., 1990. Calculation of multivariable phase diagrams: an algorithm based on generalized thermodynamics. *Am. J. Sci.*, **290**, 666–718.
- Connolly, J.A.D. and Petrini, K., 2002. An automated strategy for calculation of phase diagram sections and retrieval of rock properties as a function of physical conditions. *J. Metamorphic Geol.*, in press.
- Connolly, J.A.D. and Thompson, A.B., 1989. Fluid and enthalpy production during regional metamorphism. *Contr. Miner. Petrol.*, **102**, 346–366.
- Gasparik, T., 1985a. Experimentally determined compositions of diopside-jadeite pyroxene in equilibrium with albite and quartz at 1200–1350°C and 15–34 kbar. *Geochim. Cosmochim. Acta*, **49**, 865–870.
- Gasparik, T., 1985b. Experimental study of subsolidus phase-relations and mixing properties of pyroxene and plagioclase in the system Na_2O - CaO - Al_2O_3 - SiO_2 . *Contr. Miner. Petrol.*, **89**, 346–357.
- Hadmani, Y., Marechal, J.-C. and Arkani-Hamed, J., 1991. Phase changes and thermal subsidence in intracontinental sedimentary basins. *Geophys. J. Int.*, **106**, 657–665.
- Holland, T.J.B. and Powell, R., 1998. An internally consistent thermodynamic data set for phases of petrological interest. *J. Metamorphic Geol.*, **16**, 309–343.
- Holland, T., Baker, J. and Powell, R., 1998. Mixing properties and activity-composition relationships of chlorites in the system MgO - FeO - Al_2O_3 - SiO_2 - H_2O . *Eur. J. Miner.*, **10**, 395–406.
- Ismail-Zadeh, A.T., Kostyuchenko, S.L. and Naimark, B.M., 1997. The Timan-Pechora Basin (northeastern European Russia): tectonic subsidence analysis and a model of formation mechanism. *Tectonophysics*, **283**, 205–218.
- Kennedy, G.C., 1959. The origin of continents, mountain ranges and ocean basin. *Am. Sci.*, **97**, 491–504.
- Lobkovsky, L.I., Ismail-Zadeh, A.T., Krasovsky, S.S., Kuprienko, P.Y. and Cloetingh, S., 1996. Gravity anomalies and possible formation mechanism of the Dnieper-Donets Basin. *Tectonophysics*, **268**, 281–292.
- Lovering, J.R., 1958. The nature of the Mohorovic discontinuity. *EOS, Trans. Am. Geophys. Un.*, **39**, 947–955.
- McKenzie, D., 1978. Some remarks on the development of sedimentary basins. *Earth Planet. Sci. Lett.*, **40**, 25–32.
- Middleton, M.F., 1980. A model for intracratonic basin formation, entailing deep crustal metamorphism. *Geophys. J. R. Astr. Soc.*, **62**, 1–14.
- Naimark, B.M. and Ismail-Zadeh, A.T., 1995. Numerical models of a subsidence mechanism in intracratonic basins: application to North American basins. *Geophys. J. Int.*, **123**, 149–160.
- Newton, R.C., Charlu, T.V. and Kleppa, O.J., 1980. Thermochemistry of the high structural state plagioclases. *Geochim. Cosmochim. Acta*, **44**, 933–941.
- Podladchikov, Y.Y., Poliakov, A.N.B. and Yuen, D.A., 1994. The effect of lithospheric phase transitions on subsidence of extending continental lithosphere. *Earth Planet. Sci. Lett.*, **124**, 95–103.
- Rubie, D.C., 1990. Role of kinetics in the formation and preservation of eclogites. In: *Eclogite Facies Rocks* (D.A. Carswell, ed.), pp. 11–140. Blackie, Glasgow.
- Sobolev, S.V. and Babeyko, A.Y., 1994. Modeling of mineralogical composition, density, and elastic-wave velocities in anhydrous magmatic rocks. *Surv. Geophys.*, **15**, 515–544.
- Taylor, S.R. and McLennan, M., 1985. *The Continental Crust: its Composition and Evolution: and Examination of the Geochemical Record Preserved in Sedimentary Rocks*. Blackwell, Oxford.
- Thompson, J.B. and Waldbaum, D.R., 1969. Mixing properties of sanidine crystalline solutions. IV. Phase diagrams from equations of state. *Am. Miner.*, **76**, 493–500.
- Yamasaki, T. and Nakada, M., 1997. The effects of the spinel-garnet phase transition on the formation of rifted sedimentary basins. *Geophys. J. Int.*, **130**, 681–692.

Received 19 November 1999; revised version accepted 13 October 2000